

Hydrogen-related surface modifications of 20 nm thin straight-sided niobium nano-wires and niobium meander-films

Astrid Pundt*, Kai Nörthemann, Sönke Schmidt

University of Göttingen, Institut für Materialphysik, Friedrich-Hund-Platz 1, D-37077 Göttingen, Germany

Received 26 September 2006; received in revised form 15 January 2007; accepted 17 January 2007

Available online 31 January 2007

Abstract

Nano-wire arrays of Niobium were produced by small angle sputtering on faceted sapphire, using the self shadowing effect of the facets. A wire width of about 80 nm was adjusted, the mean (maximum) wire height was about 20 nm (30 nm), the length can be in the cm range. Meander-film morphologies of 20 nm mean (26 nm maximum) thickness were produced by conventional sputtering onto smooth sapphire substrates at elevated temperatures. The morphology of the wires was investigated with atomic force microscopy (AFM), using contact mode. Meander-films were studied by scanning tunnelling microscopy (STM).

Hydrogen loading was performed by instantaneously increasing the hydrogen gas pressure above the solubility limit. Thus, an elongated hydride could be monitored in an about 30 nm thick wire. STM studies on meander-films show the presence of cylindrical hydrides, being coherent with the matrix. This was verified by finite-element calculations. The surface morphology modification associated with these coherent hydrides disappears reversibly, as soon as the hydrogen gas pressure is reduced. This indicates that plastic deformation does not occur in thin wires and meander films.

© 2007 Elsevier B.V. All rights reserved.

Keywords: Metal hydrides; Nanostructured materials; Phase transitions; Atomic force microscopy (AFM)

1. Introduction

Thin metal nano-wires attract much interest because of their potential application as gas-sensors and as heterogeneous catalysts. Additionally, from the basic research point of view, they are interesting because of their reduced dimensionality in two directions. Metal-hydrogen (M-H) wires, especially niobium-hydrogen (Nb-H) wires, can be and have been applied as model systems to study changes of physical properties: there exist a large variety of results on bulk as well as on thin films which can be compared to the wires' properties.

For Nb-H thin films shifted solubility [2–6] and phase boundaries are reported: Song et al. [2,4] and Dornheim [6,7] determined a strong thickness dependence for epitaxial films. Laudahn et al. [5] and Pundt et al. [8] discuss the impact of micro-structure: grain boundaries, surfaces and dislocations increase the α -phase solubility limit. Additionally, stress con-

tributions affect the solubility: because of the clamping to the rigid substrate compressive stress up to several GPa arises during hydrogen absorption in the film [5,9]. This is accompanied by a strong out-of-plane film expansion which is much larger than that ($0.058 \times c_H$) of the bulk system [10,11]. For small hydrogen concentrations, the experimentally obtained expansion of $0.136 \times c_H$ is in good accordance with theoretical values obtained by using linear elastic theory [5]. An extraordinary large lattice expansion of $0.57 \times c_H$ has been reported by Reimer et al. [12], but the origin for this behavior is still unclear. For large hydrogen concentrations, plastic deformation leads to a reduced out-of-plane lattice expansion [5,13]. Plastic processes affect the vertical total film expansion which is not longer directly correlated to the lattice expansion. The discrepancy between lattice constant change and film thickness change was also observed by Rehm et al. [14]. In contrast to bulk, lattice constant and hydrogen concentration are not linearly linked for thin films [5], leading to uncertainties in the evaluation of the hydrogen concentration when the films are gas loaded [15]. This is also expected to be the case for wires. Song et al. [3,4] and Zabel et al. [10] report on the possibility to detect finite size effects

* Corresponding author. Tel.: +49 551 395007; fax: +49 551 395012.
E-mail address: apundt@ump.gwdg.de (A. Pundt).

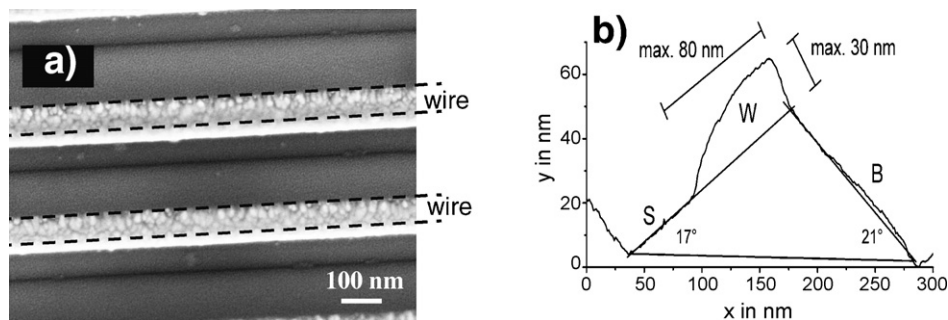


Fig. 1. (a) SEM image of Nb-wires sputter deposited onto faceted Al_2O_3 -substrates. The deposition angle was about 4° . Well-separated wires of about 80 nm width are obtained. The wire width in the image appears slightly larger because of the locally tilted substrate, thus the facet and wire sides are imaged, too. The lateral grain size within the wire is about 20 nm (grain boundaries appear grey compared to the light grains) and (b) SFM-height profile across one individual Nb-wire on a facet. The maximum wire height is 30 nm, the width is about 80 nm.

in Nb-H thin films resulting in a suppression of the hydride phase transition. According to Songs results, the phase transition should not occur at room temperature for film thicknesses below 30 nm. With a thickness of 20–30 nm for the samples studied here, hydride formation might, therefore, be absent. Up to now, hydrogen loading studies on M-H wires are limited [16], and no detailed studies have been published, yet. In this paper we study the presence and extension of hydrides forming in straight-sided Nb-wires and meander-films. This was done by monitoring the local surface morphology with AFM or STM. This method was recently established by Nörthemann et al.: for imaging the hydride forming inside of a Niobium film, they took advantage of the local lattice expansion, resulting in local surface modifications [17]. Especially, surface modifications can be attributed to hydride occurrence. The out-of-plane expansion of a clamped Nb-H-film during hydride formation with a concentration increase of $\Delta c = 0.5$ is about 6.8% of the initial film thickness while the according expansion of a free Nb-H sample is about 2.9%. Thus, the expected maximum height change for an ideally clamped wire of 30 nm maximum thickness is about 2 nm. This value exceeds the resolution limit of about 0.5 nm for the used AFM, and is well above that of the STM.

It will be shown that for the 20–30 nm thick wires and meander-films hydrides can be detected by localized surface morphology changes. Out-of-plane and in-plane expansion are in good accordance with theoretical expectations.

2. Experimental

Niobium wires were produced by sputtering onto faceted substrates that are tilted towards the incoming beam into a self-shadowing condition. These facets, with 50 nm in height and 320 nm repetition period, form by annealing an (1 0 1 0)-oriented Al_2O_3 -substrate for 24 h at 1800 K [18–20]. Meander-films consist of elongated islands above the island percolation limit. Thus, the meander film looks like a film containing deep holes.

All samples were prepared in an ultra-high vacuum (UHV) system with a base pressure of 10^{-8} Pa and argon gas (6N) pressure of about 10^{-2} Pa during sputtering. The Niobium wires were deposited at room temperature, the meander-films at 800°C , using a Niobium sputter target with 99.95 purity. Low sputter rates of about 0.2 nm/min (for wires) and 2 nm/min (for meander-films) were adjusted. After sample cooling, a cap of 1/2 of a monolayer of Pd was added to facilitate hydrogen gas sorption.

This deposition chamber is directly connected to an UHV-AFM and an UHV-STM (OMICRON), where hydrogen gas (6N) exposure up to 10^5 Pa

is possible. Maximum used hydrogen gas pressure was 10^{-2} Pa. The samples were transferred into the AFM/STM chamber right after deposition and without breaking the vacuum conditions. Surface morphology and its modifications were measured instantaneously. All investigations were performed at 20°C .

Because meander-films incessantly offer conducting surfaces they can be studied with STM. This is not possible in the case of wire arrays where conducting Niobium-surfaces alternate with non-conducting sapphire-surfaces. Thus, the surface morphology of wires was analysed with AFM in contact mode, using silicon cantilevers.

Ex situ surface morphology studies on a larger scale were performed using LEO Supra 35 scanning electron microscope (SEM). This SEM offers low kinetic electron energies of 3–5 keV and, thus, allows Al_2O_3 surface probing. For these SEM investigations exposing the samples to air could not be avoided. A typical Nb-wire morphology image is shown in Fig. 1, the deposition angle was 4° (for details see [1]). The wires are well separated and have a width of about 80 nm, while the wire length is given by that of the facets. On defect-poor substrates, local wires might span over the complete substrate length of 10 mm. The lateral grain size is about 20 nm, the mean wire thickness is approximately 20 nm and the maximum thickness is 30 nm, as can be seen from the AFM-image profile in Fig. 1(b). The wire height is not constant but it decreases towards the shadowed region.

The morphology of the meander-films is shown in Fig. 2. The mean meander-film thickness is 20 nm. The lateral meander width is about 70 nm, its length varies. The maximum measured meander height is about 12 nm (valley-to-top value), but it could be larger because the STM-tip shape might not allow non-

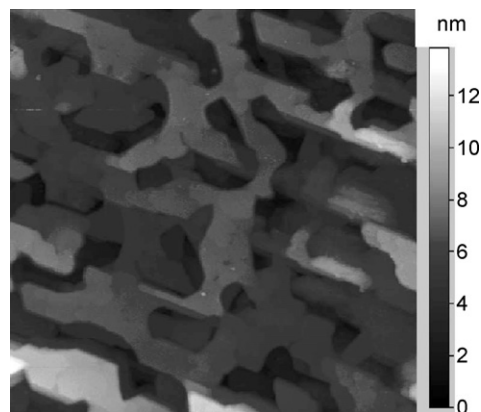


Fig. 2. STM-image ($1\ \mu\text{m} \times 1\ \mu\text{m}$) of a Nb-meander-film deposited onto a smooth sapphire substrate at 800°C . Deep valleys of 12 nm were detected—valleys can be even deeper because of the tip expansion. The meander-film is incessantly conductive. Meander-widths are of about 70 nm, the lengths vary strongly.

itoring deep valleys. Thus, the meander film height is about 20 (± 6) nm. The surface of the meanders is rather flat, just atomic steps can be detected.

3. Results and discussion

3.1. Hydrogen loading of Nb-wires

Monitoring surface morphology changes of the wires is not easy: the maximum wire thickness here was 30 nm while the expected maximum height changes are only about 2 nm. This effect is interfered by the height changes of the underlying substrate which changes each 320 nm for about 50 nm, governing the total measured height. To detect hydrogen-related surface modifications, the image of just one wire has to be taken by subtracting the associated background plane which can be adjusted at the uncovered region of the same facet. The following images are obtained by performing this background correction. The surface morphology of wires locally changes during hydrogen loading. This is shown in the AFM-images (a–c) of Fig. 3. Three subsequently taken height profiles of a wire are shown (a) before, (b) right after pressure increase to 4×10^{-2} Pa and (c) after waiting a short time. As can be seen, the maximum height is rather constant over the complete wire in (a), one height contour laterally covers the rim of the wire. A height diagram of the wire, as it is presented in Fig. 3(d), just shows one peak. After pressure increase to 4×10^{-2} Pa (b), which is well above the starting pressure for hydride formation in thin films, the height profile of the wire is higher on the left side compared to the right side of the wire. An elevated height contour line appears at the wire rim on the left side of the image. The height difference between both wire sides is about 2 nm (± 1 nm)¹, connected by a region of increasing height. The according height diagram (d) shows two distinct peaks with a separation of 2 nm (± 1 nm). When the next image is taken (c) no height difference can be detected: again, one height contour line covers the complete wire rim. However, height diagrams (Fig. 3(d)) show that the peak position of (c) is comparable to that of the left-hand peak in (b).

By reducing the hydrogen pressure to 10^{-7} Pa, one peak is detected in the height profile, at exactly the peak position of the unloaded sample (a), showing that these surface modifications are reversible. This indicates that plastic deformation does not occur during hydrogen loading and unloading in these wires.

In detail, the height diagrams originally taken from the background corrected images of Fig. 3(a–c) show a shift of the peak positions to the left side upon hydrogen loading. This effect is due to local substrate bending upon hydrogen loading of the Nb-wires. It has also to be taken into account. Details about this effect are given in Ref. [1]. The results of Fig. 3 can easily be interpreted with hydride formation in Nb-wires. The hydride expands over the wire, here entering the image from the left side, as shown in Fig. 3(b). The height difference between the right and the left wire part is about 2 nm, in good accordance with the

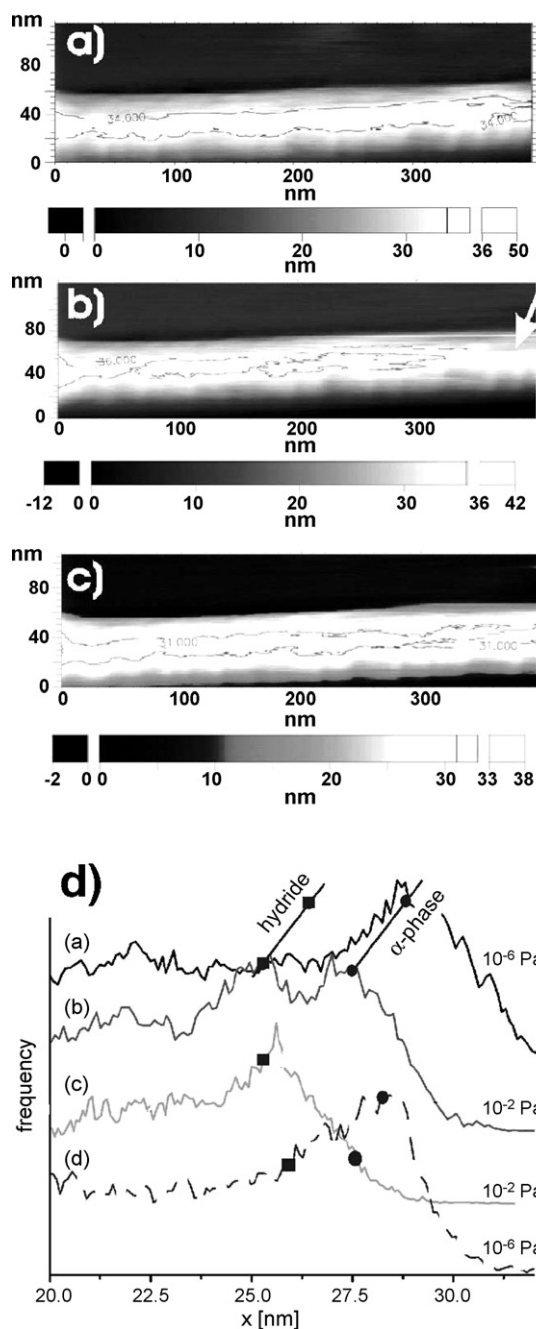


Fig. 3. Height contours of a Nb-wire (a) before and (b) right after hydrogen loading at 10^{-2} Pa. Black circles indicate the position for the α -phase height peak, black squares that for the hydride at each profile. Image (c) shows the surface morphology after 30 min hydrogen exposure. The height contours in (a) and (c) are laterally spread with uniform height, while in (b) the left part is 2 nm (± 1 nm) higher than the right part (see arrow) of the wire. In (d) all measured heights are plotted in a height diagram, verifying the appearance of two distinct peaks in case (b).

theoretical prediction. We note, that this large height change is expected when the complete underlying Nb-wire is in hydride phase.

After hydride growth, the total monitored wire is in the hydride phase, resulting in one peak again. By this, hydrogen desorption leads to a recovery of the original height, verifying a reversible morphology change. Because of this reversibility we

¹ The large error accounts for the substrate bending effect which can be different for the different substrate parts and results in an overestimation of the peak splitting. For details, see Ref. [1].

suggest that hydride precipitates are coherent in the 30 nm thick wires.

We note that from these measurements it cannot finally be judged if the high concentration phase forms by phase transformation (correlated to the passing of the miscibility gap) or by continuous concentration increase (correlated to the simple solid solution). The detected two-phase state might also be of kinetic origin: inhomogeneous loading conditions might result in time dependent local concentration differences washing out after the equilibrium condition of the solid solution is reached. But, according to many earlier STM-measurements on comparable Nb-samples (with areas up to $3\mu\text{m} \times 3\mu\text{m}$), inhomogeneous hydrogen loading has never been detected within the solid solution phase. For example, Nörthemann et al. [17] reported on a uniform thickness increase upon H-loading of thin films. Thus, we conclude to have monitored hydride formation and phase transition in the 20–30 nm thin Nb-wire. This finding is different to the results of Song et al. who reported on a vanishing phase transition for thin films [3,4].

3.2. Hydrogen loading of Nb-meander-films

Hydrogen-related surface morphology changes of 20 nm thin meander Nb-films could be imaged by using the difference image technique: two subsequently taken STM-images of the same area are subtracted thus giving the height changes. Such a difference image is shown in Fig. 4. The hydrogen gas pressure was 10^{-7} Pa for the first image, and 10^{-3} Pa for the second one. As can be seen, the complete difference image is elevated compared to the former image, resulting in a uniform grey scale. This constant elevation can be understood by taking into account homogeneous hydrogen absorption within the α -phase region. Additionally, bright ellipsoidal regions can be detected. They are elevated by about 1.1 nm (± 0.2 nm) compared to the base level of the according terraces. Height profiles of one region also show a lateral expansion of about 3.0 nm (± 1.5 nm) to each side. This can only be interpreted with the local formation of hydrides and phase transition. Such local-

ized hydrides cannot be understood by homogeneous hydrogen absorption, as it would be expected when a phase transition is suppressed.

Thus, the presence of hydrides embedded in α -matrix verifies the presence of a phase transition in 20 nm meander films.

The transition region between the ellipsoidal region and the adjacent terrace surface spreads over several nm. The increase angle is about $2.5 (0.4)^\circ$. This can only be understood in case that the hydrides in 20 nm thin meander-films are coherent to the α -phase matrix. An incoherent precipitate would result in a much steeper transition—when a buried incoherent precipitate were present, the transition region would be expanded but the maximum height increase would be reduced, simultaneously. This is not the case. Therefore, we suggest that coherent precipitates form in the 20 nm thin Nb-meander-films. To investigate the reversibility of precipitation, unloading studies of Nb-H meander-films are planned.

3.3. Calculations of surface morphology changes upon coherent hydride formation

In this paragraph the measured height changes upon coherent hydride formation in wires shall be explained with help of finite-elements-calculations. Height changes are slightly smaller than what is expected from calculations of the ideally clamped thin film, using linear elastic theory. Out-of-plane expansion of about 7% of the sample thickness was calculated. This would result in 1.4 nm height increase. As it was shown, hydride formation in 20 nm Nb-meander-films leads to surface morphology changes of up to 1.1 nm.

Since the latter result is precise within 0.2 nm, this value slightly differs from the calculated one. The difference results from the following reasons: (1) For the thin film calculations, in-plane expansion was suppressed. But wires should expand perpendicular to the wire axis, at least in the upper regions, as reduced lateral stress leads to reduced out-of-plane expansion. (2) Additionally, our experimental results suggest coherent hydrides. Thus, coherency stress between the α -matrix and the

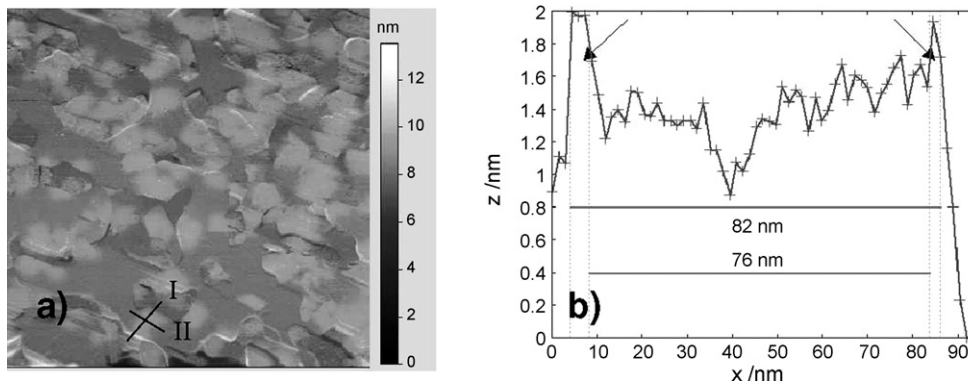


Fig. 4. (a) Difference images of two STM-images ($1\mu\text{m} \times 1\mu\text{m}$) taken at the same region of meander Nb-films. The first image is taken at 10^{-7} Pa (α -phase of bulk Nb-H), the second at 10^{-3} Pa (hydride phase of bulk Nb-H). Homogeneous hydrogen absorption leads to constant background elevation. Localized ellipsoidal regions verify the presence of hydrides. The height difference is about 1.1 (± 0.2) nm. (b) A height profile across such an ellipsoidal region shows peaks at the both sides (marked with black line I); they can be understood with a lateral expansion of 3 (± 1.5) nm in this region. The profile along the black line II is presented in Fig. 5(b).

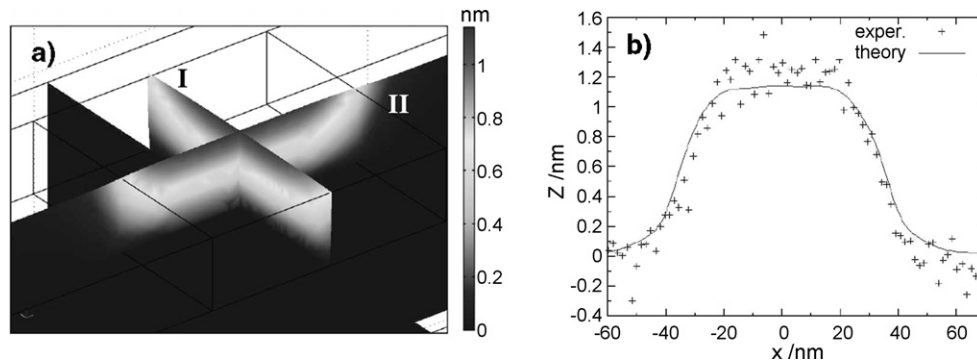


Fig. 5. (a) Cross-sections of Finite elements calculations of the film expansion upon hydride formation in a Nb wire (20 nm thickness, 70 nm width and 300 nm length) deposited on a sapphire substrate, (I) perpendicular to the wire axis and (II) along the wire axis. The hydride is approximated by a block of $70 \text{ nm} \times 70 \text{ nm} \times 20 \text{ nm}$. Maximum vertical expansion of 1.1 nm can be seen as well as a vertical expansion. The height profile in part (b) compares the experimental data along the marked line II in Fig. 4(a) and the theoretical calculations results along the wire axis (a) along marked line (II).

hydride should reduce the total height of the hydride. (3) Furthermore, one also has to discuss the presence of cylindrical hydrides with vertical extension smaller than the film thickness which would also lead to a reduced height change.

To address the geometrical argument (1) and the interpretation (2), we performed finite-element calculations using the COMSOL Multiphysics software equipped with the structure module. It allows calculating the wire- or meander-shape when a coherent hydride is formed. For simplicity, the wire geometry was set to 20 nm thickness, 70 nm width and 300 nm length. The coherent hydride is approximated by a block of $70 \text{ nm} \times 70 \text{ nm} \times 20 \text{ nm}$. Volume expansion is accounted for by subsequent straining of the block by 2.9% ($\Delta c \times \delta = 0.5 \times 5.8\%$, with δ expansion factor of Nb-H). Elastic constants and Poisson's ratio of bulk Nb and sapphire were applied for the wire and the substrate, subsequently [21]. Border conditions were set as follows: no expansion was allowed at the substrate-wire interface. At this interface, the wire is ideally clamped and in-plane substrate expansion is suppressed. No lateral expansion was allowed at both wire borders in y-direction (which was the wire axis).

The calculations give a wire expansion as it is shown in Fig. 5. At the wire/substrate interface no expansion occurs because of the ideal clamping to the rigid substrate. But elevated wire regions expand and appear lighter compared to the substrate. A total lateral x -expansion of 2.4 nm is calculated, with 1.2 nm on each side. In vertical direction, the wire expands by about 1.1 nm. Because of coherency stress, the height increase between the hydride and the α -phase spreads over several nm. The height increase in this transition region has a slope of about 2.4° (parallel to the wire direction). The calculated result is in good accordance with the experimental observation. This is shown in Fig. 5(b), where we plotted an experimental height profile taken (from Fig. 4(a)) and the calculated height profile (for the coherent precipitate that exists right through the complete wire). The calculations describe the experimental data quite accurately, both in vertical direction and for the slope. Thus, the presence of coherent precipitates being smaller than the wire thickness (case 3) cannot be verified.

4. Conclusions

Twenty to thirty nonometers thin Nb-wires and -meander-films were studied by STM/AFM technique to monitor surface morphology changes upon an increase of the hydrogen partial pressure. Localized surface morphology changes were found in both types of samples. For wires, the hydrides were detected by a local height increase of about $2 (\pm 1)$ nm. Hydrogen partial pressure reduction results in reversible change of the surface morphology. This can be interpreted with the dissolution of precipitates that are formed coherently in the sample.

For meander films, localized ellipsoidal regions were detected that were elevated by about $1.1 (\pm 0.2)$ nm above the base level. They were explained by the presence of hydrides inside the meander-film. The transition region between the elevated ellipses and their neighboring regions is characterized by a moderate height decrease with a slope of only 2.3° . Therefore, precipitates were suggested which are coherent with the Nb-matrix.

Finite element calculations on a coherent precipitate with 20 nm thickness match the experimental data accurately.

To summarize, the results presented in this paper suggest the presence of phase transition in Nb-H wires and meander-films of 20–30 nm thickness. These experimental results are different from those expected from the model of the vanishing phase transition for Nb-samples in the range of 30 nm [3,4].

Acknowledgement

Financial support of the DFG via SFB602 is gratefully acknowledged.

References

- [1] S. Schmidt, A. Pundt, submitted for publication.
- [2] J. Steiger, S. Blässer, A. Weidinger, Phys. Rev. B 49 (1994) 5570.
- [3] G. Song, M. Geitz, A. Abromeit, H. Zabel, Phys. Rev. B 54 (1996) 14093.
- [4] G. Song, A. Remhof, K. Theis-Bröhl, H. Zabel, Phys. Rev. Lett. 79 (1997) 5062.
- [5] U. Laudahn, A. Pundt, M. Bicker, U.v. Hülsen, U. Geyer, T. Wagner, R. Kirchheim, J. Alloys Comp. 293–295 (1999) 490.

- [6] M. Dornheim, Ph.D. Thesis, University of Göttingen, 2002.
- [7] M. Dornheim, R. Kirchheim, A. Pundt, in preparation.
- [8] A. Pundt, R. Kirchheim, *Ann. Rev. Mater. Res.* 36 (2006) 555–608.
- [9] A. Pundt, *Adv. Eng. Mater.* 6 (2004) 11–21.
- [10] H. Peisl, Lattice strains due to hydrogen, in: G. Alefeld, A. Völkl (Eds.), *Hydrogen in Metals I*, Springer-Verlag, 1978.
- [11] H. Zabel, A. Weidinger, *Comments Cond. Mat. Phys.* 17 (1995) 239.
- [12] P.M. Reimer, H. Zabel, C.P. Flynn, A. Matheny, K. Ritley, *Z. Phys. Chem.* 181 (1993) 929.
- [13] A. Pundt, M. Getzlaff, M. Bode, R. Wiesendanger, R. Kirchheim, *Phys. Rev. B* 61 (2000) 9964.
- [14] Ch. Rehm, H. Maletta, M. Fieber-Erdmann, E. Holub-Krabbe, F. Klose, *Phys. Rev. B* 65 (2002) 113404.
- [15] A. Pundt, U. Laudahn, U.v. Hülsen, U. Geyer, M. Getzlaff, M. Bode, R. Wiesendanger, R. Kirchheim, *Mat. Res. Soc. Symp. Proc.* 594 (2000) 75.
- [16] F. Favier, E.C. Walter, M.P. Zach, T. Benter, R.M. Penner, *Science* 293 (2001) 2227.
- [17] K. Nörthemann, R. Kirchheim, A. Pundt, *J. Alloys Comp.* 541 (2003) 356–357.
- [18] M. Huth, K.A. Ritley, J. Oster, H. Dosch, H. Adrian, *Adv. Funct. Mater.* 12 (2002) 333.
- [19] C. Herweg, Ph.D. Thesis, Universität Göttingen, 2005.
- [20] A. Wesphalen, H. Zabel, K. Theis-Bröhl, *Thin Solid Films* 449 (2004) 207.
- [21] D.R. Lide (Ed.), *Chemical Rubber Company Handbook of Chemistry and Physics*, 79th ed., CRC Press, Boca Raton, Florida, USA, 1998.